

# Raman identification of single nucleotides flowing through permeable plasmonic films

Received: 17 December 2024

Accepted: 10 September 2025

Published online: 14 October 2025

 Check for updates

Kirill Khabarov<sup>1</sup>, Maria Blanco Formoso<sup>1</sup>, Iliaria Micol Baldi<sup>1,2</sup>,  
Forough Khozayemeh Sarbishe<sup>1</sup>, Riccardo Marongiu<sup>1</sup>, Giulia Bruno<sup>1</sup>,  
Bikash Bhandari<sup>3</sup>, Veronica Storari<sup>4</sup>, Henri Haka<sup>4</sup>, Michele Dipalo<sup>1</sup>,  
Paolo Canepa<sup>2</sup>, Francesco Gentile<sup>5</sup>, Nick Goldman<sup>3</sup>, Federica Villa<sup>4</sup>,  
Francesco Tantussi<sup>1,6</sup>✉ & Francesco De Angelis<sup>1,6</sup>✉

Surface-Enhanced Raman Scattering has been studied for decades as a recognition technique due to its high sensitivity and discriminative power, particularly in biological applications. Inspired by nanopore sequencing technology, we developed a plasmonic device capable of operating in a flow-through configuration to detect individual molecules passing through plasmonic hotspots. This device is a permeable plasmonic film, through which single molecules are sequentially delivered via electrophoresis, while Raman spectra are recorded in real-time. A very effective light-matter coupling, combined with the ultrasmall size of plasmonic spots, enabled access to angstrom spatial and microsecond temporal scales compatible with polymer sequencing. We successfully slowed the translocation process and captured Raman spectra of the four nucleotides at a time resolution down to 20  $\mu$ s under our experimental conditions. We achieved a discrimination accuracy of 89% at the single-molecule level. Also, we demonstrated a spatial resolution on the order of a few nucleotides, suggesting the potential for sequencing applications.

Surface-Enhanced Raman Scattering (SERS) has been extensively studied and utilized over the past 30 years, producing significant advancements across various research fields. Among its many applications, SERS has emerged as a powerful tool for investigating biological analytes, enabling the analysis of a broad spectrum of molecules such as proteins, lipids, nucleic acids, and metabolites without the need for labelling. Raman Spectroscopy offers molecular “fingerprints” with sensitivities that can reach the single-molecule level, a milestone achieved by numerous laboratories<sup>1–3</sup>. This success has led to the proposal of many practical applications. However, despite considerable efforts, the impact of SERS in real-world applications remains limited due to several challenges, as outlined in technical reviews<sup>4,5</sup>.

One of the key challenges in biomolecule discrimination is that, although SERS can achieve single-molecule sensitivity, it captures the spectrum of the molecule as a whole. However, molecular identity is linked not merely to the individual components but to their specific spatial arrangement. This is especially critical in biological contexts, where nucleic acids and proteins consist of sequences made up of just four and twenty types of units, respectively. For example, consider two short DNA sequences like GAT-TACA and CATAGAT. Despite being distinct sequences, their Raman spectra would be remarkably similar, making them difficult to differentiate when their spectra are recorded in their entirety. In contrast, if the spectra of individual nucleotides could be recorded

<sup>1</sup>Istituto Italiano di Tecnologia, Genova, Italy. <sup>2</sup>Department of Physics, University of Genova, Genova, Italy. <sup>3</sup>European Molecular Biology Laboratory, European Bioinformatics Institute (EMBL-EBI), Wellcome Genome Campus, Hinxton, Cambridgeshire CB10 1SD, UK. <sup>4</sup>Dipartimento di Elettronica, Informazione e Bioingegneria, Politecnico di Milano, Milano, Italy. <sup>5</sup>Nanotechnology Research Center, Department of Experimental and Clinical Medicine, University of “Magna Graecia” of Catanzaro, Catanzaro, Italy. <sup>6</sup>These authors contributed equally: Francesco Tantussi, Francesco De Angelis.

✉ e-mail: [francesco.tantussi@iit.it](mailto:francesco.tantussi@iit.it); [francesco.deangelis@iit.it](mailto:francesco.deangelis@iit.it)

sequentially (one by one along the DNA chain), an accurate identification of the molecule would be feasible.

Such an identification strategy through sequential reading of molecular fragments is already employed in other fields such as Mass Spectrometry<sup>6</sup> and nanopores sequencing technologies<sup>7,8</sup>. The latter involves driving DNA molecules through biological or solid-state nanopores via electrophoresis. By measuring the electrical current during molecular translocation, it is possible to identify specific nucleotides and determine the DNA sequence. Despite the success of these technologies, challenges remain, such as improving accuracy and achieving ultra-long DNA reads. Additionally, adapting these methods to proteins with their post-translational modifications (currently estimated at around 400 modifications) or RNA with its post-transcriptional modifications (estimated at around 170) poses significant difficulties<sup>9</sup>. These challenges look enormous, and currently, only polypeptide looks reachable, thanks to the effort of a huge community<sup>8</sup>. To achieve the necessary sensing accuracy and discrimination power, new sensing modalities or their integration with existing technologies are required<sup>7</sup>. Given the richer information content of Raman fingerprints compared to electrical readouts, SERS presents a promising opportunity to bridge this gap. Some remarkable results in this direction were already achieved by Wang's group on the identification of proteins and their single-point mutations by exploiting a plasmonic nanopore integrated in a capillary tip<sup>10</sup>. Furthermore, plasmonic nanopores have been successfully integrated with SERS at the single-molecule level, as demonstrated by Van Dorpe's group, where real-time monitoring of single-molecule nucleotides interacting with a plasmonic hotspot was achieved<sup>11</sup>. Other early important results on plasmonic membranes were also achieved by De Angelis's group on DNA identification and detection of single nucleotides<sup>12–14</sup>. However, for the approach to evolve further, advanced plasmonic devices and Raman sensing modalities must be developed to reach spatial and temporal resolution comparable to those achieved in the field of nanopores with electrical readouts.

In this work, we make a step toward a method for identifying the molecular constituents in biopolymers by Raman sequential readout. We developed cost-effective, permeable plasmonic films embedded with ultrasmall metallic nanopores through which molecules can flow via electrophoresis. Such permeable films provide a strong light-matter coupling in ultrasmall plasmonic hot spots that lead to giant Raman signals through SERS amplification. The latter, combined with the ultrasmall size of plasmonic spots, allows the method to access extreme spatial and temporal resolution conventionally not accessible to SERS, namely a few angstroms and tens of microseconds. In such devices, molecules are not permanently adsorbed onto the metal surface but remain mobile in wet conditions. They are detected in a flow-through scheme, translocating through the nanopore within 20–40  $\mu$ s. This is at least 10 times slower compared to the translocations in regular solid-state nanopores with electrical readout<sup>15</sup>. To capture such an ultrafast dynamic, we take advantage of the latest generation of Single-Photon Avalanche Diode (SPAD) camera and then use Machine Learning to analyse the data. We successfully recorded and distinguished the spectra of the four nucleotides passing through the film at a single-molecule level and nanomolar concentration. We achieved a classification accuracy of single-nucleotide translocation exceeding 89% at a single-molecule level and exceeding 99% when averaging on >10 events. Finally, using simple single-stranded DNA (ssDNA) oligos, we demonstrated a spatial resolution along the ssDNA backbone of a few nucleotides. While further investigations and optimizations are necessary, these results clearly demonstrate that the Raman sequential readout can meet the minimum requirements for polymer sequencing. Importantly, the simplicity of this methodology, coupled with the use of readily available technologies, makes it particularly well-suited for translational applications, representing a long-sought goal within the SERS community. Compared to electrical

readouts, this method's primary advantages lie in i) its potential ability to discriminate a broader range of molecular constituents beyond the four nucleotides; ii) no need for labelling or sophisticated biochemistry; iii) no need for complex reference databases for base or amino acid (AA) identification; iv) simple and inexpensive fabrication process for devices that, in contrast with biological pores, are robust and easy to preserve and transport<sup>16</sup>.

## Results

### Plasmonic device characterization

Agarose gel, commonly used in 2D gel electrophoresis, provides an economical and widely adopted method in molecular biology laboratories. Biomolecules such as proteins, nucleic acids, and metabolites migrate through the gel under an electric field, allowing their separation based on their molecular weight. We developed a permeable plasmonic device by depositing a thin film of silver (12 nm) on top of a layer of agarose gel (5  $\mu$ m). To improve adhesion between silver and agarose, we deposited a layer of titanium (5 nm) in between (for more details, see Supplementary Note 1). Due to the porous nature of agarose, silver forms a polycrystalline structure with nanogaps in between single crystals (Fig. 1a). This structure exhibits plasmonic properties similar to granular metal films, with hot spots forming between the grains and an enhancement that depends on their separation distance<sup>17,18</sup>. The electrophoretic field applied across the layers first delivers the molecules through the gel in a way similar to conventional electrophoresis and then through the nanogaps of the silver film. In our experiments, the electrophoretic field was introduced with a power supply set to 30 mV.

The nanoholes and nanoslits are shown on the SEM image of the plasmonic device surface (Fig. 1b) and, for the sake of simplicity, will be called nanopores. We estimated the size distribution of the nanopores, i.e. the width of nanoslits and diameters of nanoholes, by analysing at least 400 of them on SEM images (Supplementary Note 2, Fig. 1c). The size of nanopores varies from 1 nm (the minimum value we can observe) up to a maximum of 15 nm. By fitting the nanopore size distribution, we determined that the most prevalent size corresponds to 3.8 nm. This is an ideal value for plasmonic detection of biopolymer translocating through the permeable film. In fact, the diameter of DNA and proteins, upon unfolding and linearization, is in the order of 1–2 nm. Hence, a nanopore of 3.8 nm is ideal to let the molecule pass through while keeping tight contact between the metallic surface and the molecule itself. Such tight contact promotes an effective coupling between plasmons and molecules to achieve a huge Raman enhancement, as we will show thereafter. Notably, the pore size analysis was conducted on a dry sample, whereas translocation experiments were performed in buffer solutions, where agarose is expected to swell, potentially affecting nanopores. To investigate this effect, we conducted Atomic Force Microscopy (AFM) on the device immersed in water. However, no significant increase in nanopore dimensions was observed, suggesting that the swelling does not alter the functionality of devices. This is likely caused by the gel being constrained by a non-deformable membrane and confined within a 500 nm well, limiting its ability to expand (Supplementary Note 3, Figure S1).

### Ultrafast SERS detection with SPAD camera

The spectral response of the plasmonic film is reported in Fig. 1d (see methods in Supplementary Note 4). The optical spectra demonstrate a wide attenuation band with the maximum corresponding to 465 nm and remaining high in the whole visible range. To further understand Raman amplification, we investigated the intensity of the Raman emission and Signal-to-Noise Ratio (SNR) for different wavelengths, namely 488, 514, 532, 633, 785 nm. The results are reported in Figure S2. We found that the optimal SNR was achieved at  $\lambda=532$  nm. All the following experiments were carried out with this wavelength. It is well known that radiation at this wavelength causes fluorescence of

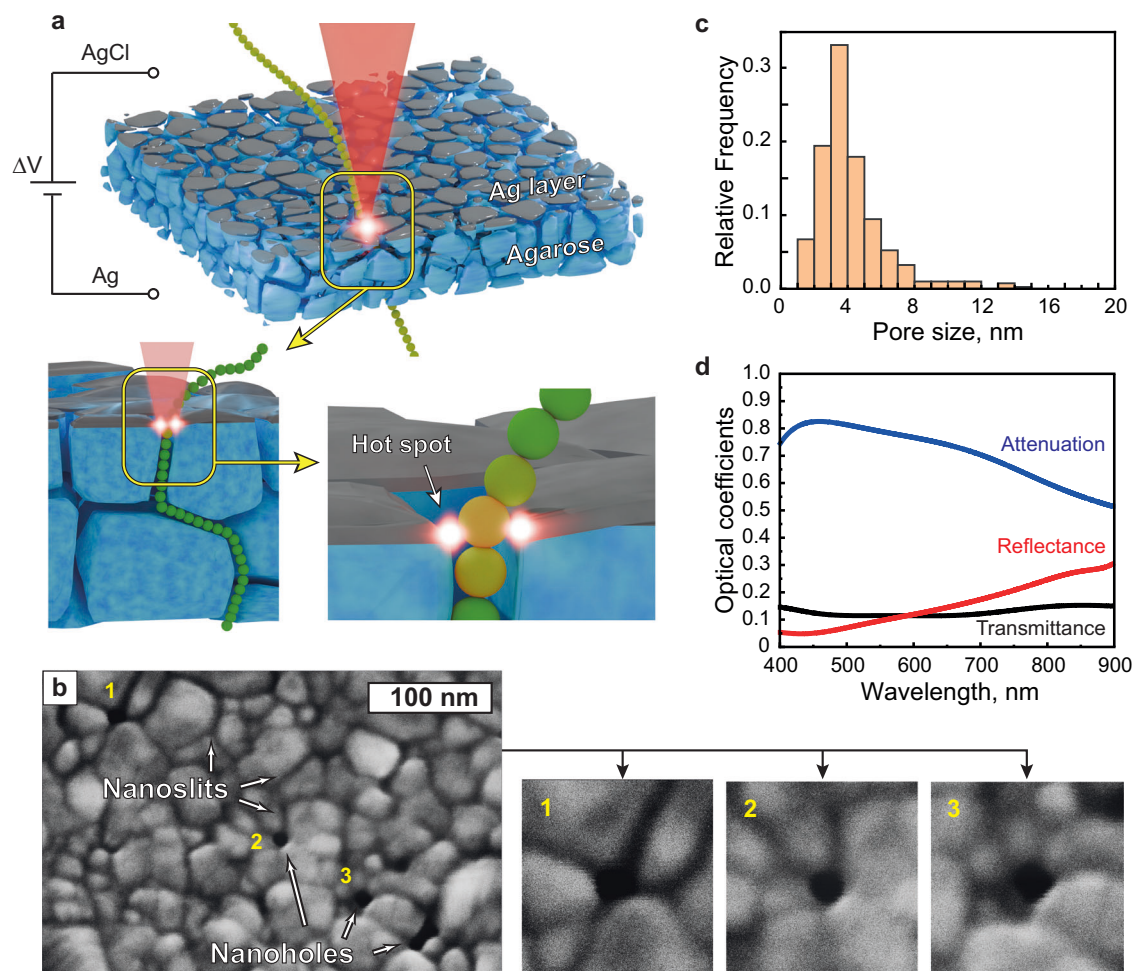


**Fig. 1 | Sample overview and characterization.** **a** Permeable plasmonic device model with an intuitive representation of a linear molecule passing through a plasmonic hot spot on top of a silver film. **b** SEM image of the silver surface of the

device with enlarged SEM images of various nanopores on it (1-3). **c** Size distribution of the nanopores on the surface of the device with a mode equal to 3.8 nm. **d** Optical spectra of the plasmonic device in NaCl 150 mM aqueous solution.

organic analytes. In the following experiments, however, its influence was negligible compared to the Raman signals collected. This is attributed to the well-known quenching effect that occurs in proximity to the metallic surface<sup>19</sup>.

Following the translocation dynamic into nanopores is necessary to reach a temporal resolution on the microsecond time scale. With this aim, we mounted a  $64 \times 32$  pixels SPAD camera (Micro Photon Devices – MPD, SPC3 Series) on a Raman microscope (InVia Renishaw) and customized software (Figure S3). Technical details on the camera are provided in Supplementary Notes 5 and 6. Then, we combined the Raman detection system with electrophoretic delivery of molecules into the permeable films. The general scheme of the setup is provided in Figure S4. Other details on the setup preparation and sample installation are provided in Supplementary Note 5. It should be noted that few studies exist on SERS emission on the microsecond timescale, and furthermore, they rely on molecules adsorbed on plasmonic surfaces in dry conditions or even in a vacuum. In this work, we investigate the ultrafast dynamic of single small molecules translocating in the proximity of ultrasmall plasmonic spots. Furthermore, molecules are not adsorbed onto the metal surface but are free to move in wet conditions. Very little is known in this regard. The most closely related fundamental studies of extremely confined plasmonic spots (sometimes called “picocavities”) have been carried out by the groups of Baumberg and Aizpurua<sup>20,21</sup> and, regarding ultrafast SERS dynamics, by the group of Brolo and Lyndquist<sup>22,23</sup>.

### Translocation of single nucleosides

To characterize the system performance, we have chosen single nucleosides (nucleotides without a phosphate group) and ssDNA oligos as probe molecules (Supplementary Note 7). Importantly, we intentionally focused the analysis on very short molecules to limit the variability of the experiments and facilitate interpretation. Longer molecules may translocate with more complex dynamics, leading to results that are difficult to interpret in the context of a developing nanopore technology, where reference literature is limited. In contrast, short molecules of a few tens of bases behave like rigid rods, with lengths that are shorter than or comparable to pore sizes. It follows that they can pass through the pore in different orientations, either longitudinally or transversally relative to the pore. However, this is the only uncertainty to consider when analysing the data.

In the first experiment, we used single nucleosides (adenosine (A), cytidine (C), thymidine (T), and guanosine (G)) diluted to the concentration of 1 nM. At that concentration, molecules translocate through the membrane one at a time, minimizing the probability of simultaneous translocation of multiple molecules through different nanopores. This assumption is supported by the calculated interval between consecutive translocations (Fig. 2c, Figure S5) that is at least 19 times longer than the average translocation time of a single molecule 20–40  $\mu$ s (Fig. 2a). Among the molecules used, no significant differences were observed in the translocation time. Supplementary Video 1 provides an example of the data collection process. The

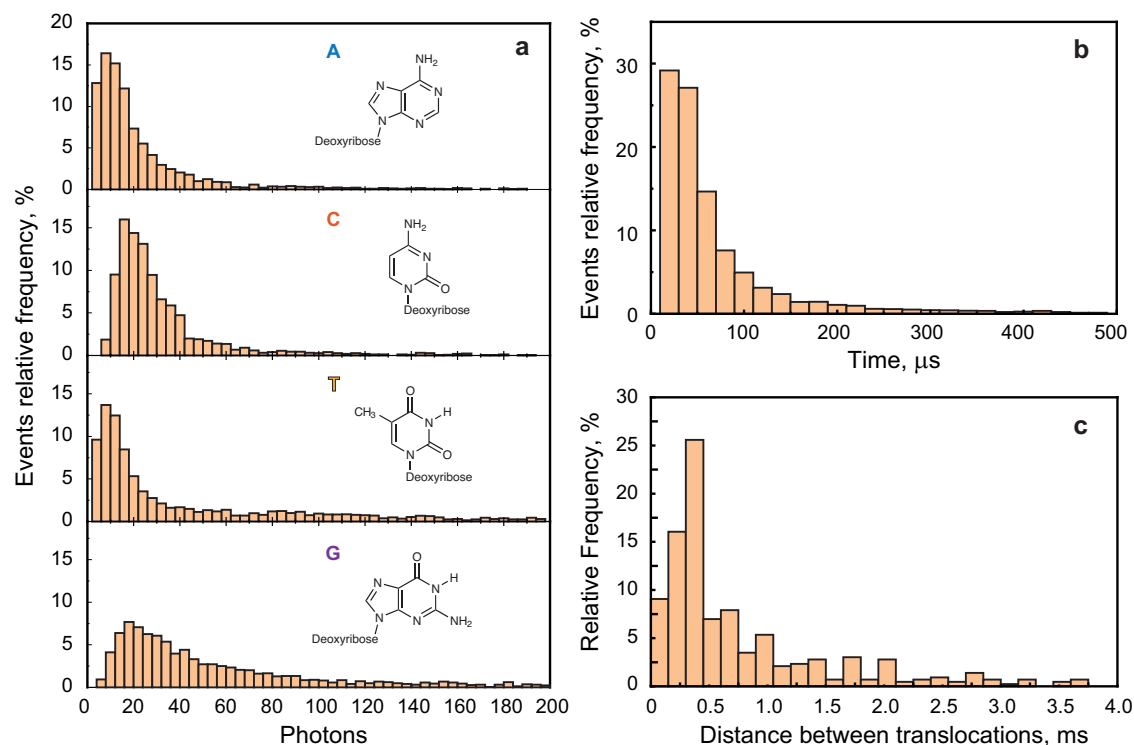


**Fig. 2 | Translocation statistics for A, C, T, and G at 1 nM concentration acquired with 20  $\mu\text{s}$  time resolution. a** Distributions of photons emitted during detected translocations, **b** Translocation time distribution, and **c** Distribution of time intervals between neighbouring translocations.

primary objective of this experiment was to characterize the system's performance in terms of translocation time and SNR and to demonstrate that single molecules can be efficiently delivered through the permeable plasmonic film similar to a solid-state nanopore. The photon count distributions for all investigated nucleosides are presented in Fig. 2b. Under the experimental conditions adopted, we observed similar photon Raman scattering rates, with a maximum value ranging from 10 to 20 photons per molecule above the average background noise level of 13 photons per 64 camera pixels per measurement (Figure S6). Furthermore, the overall efficiency of our setup can be estimated as 10% at maximum by considering efficiencies of lenses, camera, captured spectral range, and so on. Hence, the real number of Raman photons is much higher than the one we collected with the current setup, and the room for improvement is massive. The distribution of translocation time, reported in Fig. 2a, shows that in 56% of the detected events, the molecules translocate within 20–40  $\mu\text{s}$ . Such a value is at least 10 times larger than that usually achieved in solid-state nanopores. And indeed, with standard buffers (NaCl, KCl) the translocation time is typically lower than 1  $\mu\text{s}$  per base<sup>24,25</sup>. In our case, such a low speed<sup>15</sup> may be explained by the presence of the gel, that slows down the molecules and reduces the intensity of the electrophoretic field in the silver pore. Also, the present method works for very low electrical bias (30 mV) that keeps the molecular speed slow. A minor part of events (~10%) exhibited translocation times longer than 100  $\mu\text{s}$ . These events most probably correspond to the molecules translocating through the pore in a “stop-and-go” manner along the inner Ag surface of the pore, performing a stronger Raman signal due to the closer exposure to plasmonic hot spots.

### Molecular fingerprints and classification accuracy

In Fig. 3 we report the average spectra of single nucleosides. Even though the spectral resolution corresponds to  $\sim 10 \text{ cm}^{-1}$ , hence lower than that typically used in Raman Spectroscopy ( $\sim 2 \div 4 \text{ cm}^{-1}$ ), key differences between the Raman spectra of the bases can still be observed. Remarkably, the spectra of Fig. 3 are achieved by averaging a few

hundred single translocation events. To further assess the information content of the recorded spectra beyond the average, we utilized Principal Component Analyses (PCA)<sup>26</sup>. Results are presented in Fig. 3b and show that all the nucleoside's single translocation spectra are separated from each other with a minimum overlap. A detailed description of the method is provided in Supplementary Note 8.

We also estimated the classification accuracy using the first 10 principal components (PC) of Random Forest algorithm that retains the higher explained variance of the dataset and a 70/30 train-test split. Over 10 iterations with randomly selected test sets, the Random Forest model achieved an average accuracy of 89% for the four nucleosides' classification (other statistical results are presented in Figure S7). Despite such a structural similarity at a molecular level, the analyses gave out high accuracies, demonstrating the strong performance of the method in distinguishing the four classes. Another typical limit of SERS is the spectral fluctuation of Raman peaks that rapidly change position along the time<sup>23</sup> making identification of the molecule difficult. The data we collected show that when molecular moieties are recorded one by one, the Raman fingerprint is robust enough to compensate for peaks' fluctuation and allow clear identifications in label-free mode, a pivotal point for next-generation biosensors<sup>27</sup>.

To validate our approach, we repeated the experiment on the same membrane, using a mixture of two non-complementary nucleosides (A and C). First, we translocated A alone and then added C molecules and recorded the translocation of the mixed solution. We analysed the data by PCA and the results are reported in Fig. 3c. PCA analysis revealed distinct A and C clusters when running together (blue points). As a control we analysed the data of A running alone (orange points) that correctly overlap with the A cluster. Notably, these data unambiguously demonstrate that the majority of molecules pass through the pores one by one. In fact, a significant overlap between the clusters would indicate a mixed spectrum resulting from the simultaneous passage of A and C, which is not observed in Fig. 3c. Additionally, to assess the repeatability of the data across different nanopore

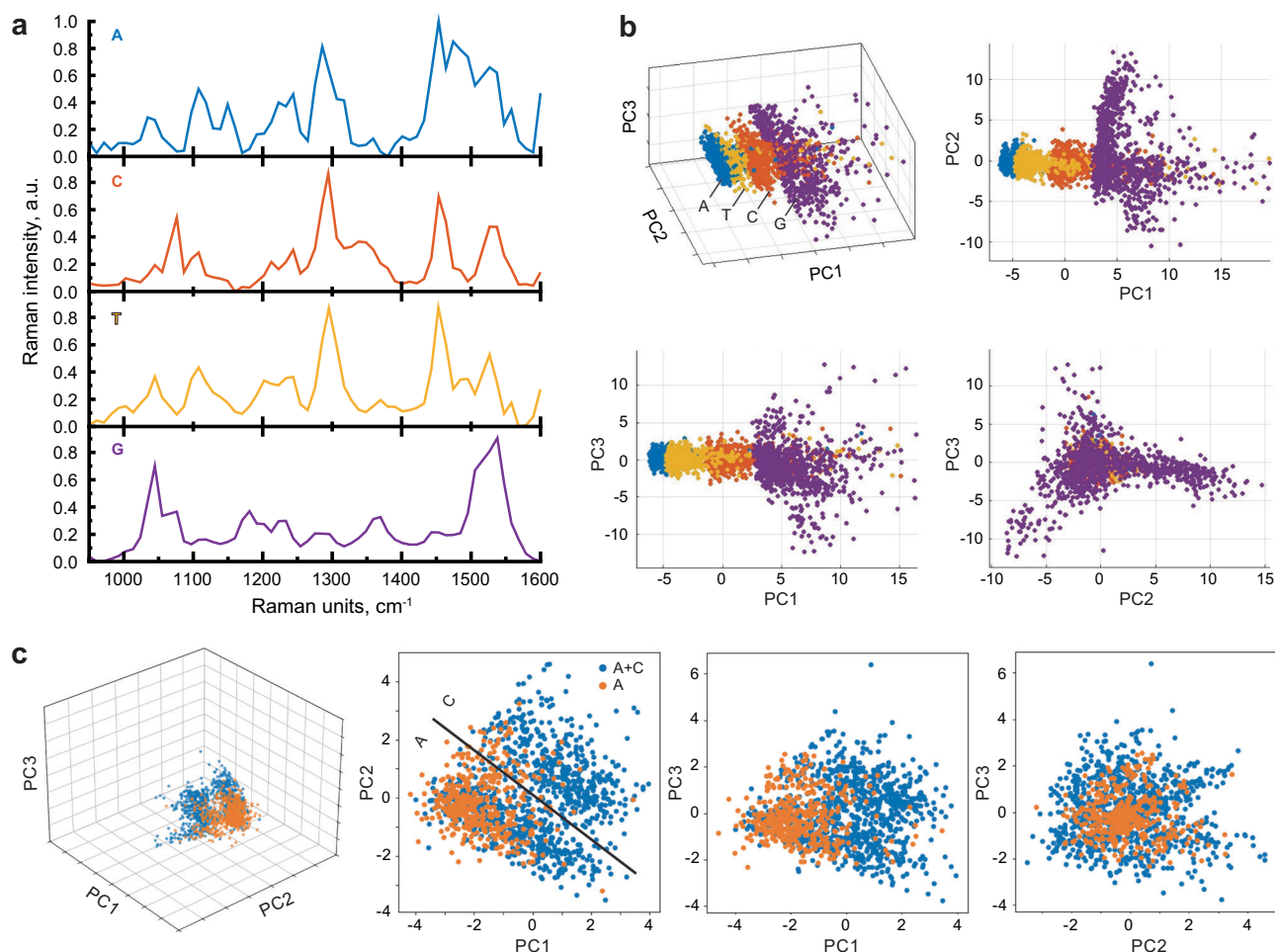


**Fig. 3 | SERS performance of A, C, T, and G acquired with the SPAD camera.** **a** Averaged SERS spectra. **b** PCA: the score plot of the distribution for the datasets of the four nucleosides. **c** PCA: the score plot of the distribution for the experiment with consecutive addition of C molecules to A molecules solution. The 2D plots

depict relationships between the main components (PC1, PC2, PC3). The 3D scatter plots of the first three PC visualize the overall clustering and separation of the datasets.

membranes, we conducted separate runs using 1 nM of the A molecule. The resulting data clusters closely together, supporting the robustness of our approach (Figure S8).

### Towards oligonucleotide sequencing

The data presented above suggest that the method can achieve performance comparable to state-of-the-art approaches in terms of sensitivity, temporal resolution, and discrimination power. However, when the nucleotide is part of a real sequence, i.e., of DNA or other biopolymers, an extreme spatial resolution is also needed to resolve the relative sequence of the moieties. In fact, the length of a single nucleotide along the polymeric chain is only 0.34 nm. To investigate this aspect and resolve the submolecular structure, we conducted a series of three experiments using ssDNA oligos. First, we studied the sequence GGGGAGGGG (G4AG4), in analogy with our previously published work<sup>14</sup>. We then examined the A5C5 (AAAAACCC) oligo sequence, and finally, a hybrid quasi double-stranded construct A5C(CG)4AG4 formed by linking G4AG4 and A5C5. While the analysis in Fig. 3 focused on distinguishing between different molecules, the current experiment aimed to resolve structural differences within individual molecules. Significant results were obtained with both A5C5 and A5C(CG)4AG4 molecules, which contain two and three blocks, respectively. To demonstrate the resolving power of our method, we analyzed the data at the level of individual frames. This frame-by-frame analysis poses a greater challenge in terms of both SNR and

computational complexity, making basic PCA insufficient. Therefore, we employed Uniform Manifold Approximation and Projection (UMAP)<sup>26</sup>, a dimensionality reduction technique well-suited for high-dimensional spectral data. Figure 4a, c illustrates individual translocation events with long dwell times, enabling visual identification of molecular blocks directly from the waterfall plots without the need for complex analysis. Such long translocations show distinct spectra with sharp transitions between molecular blocks. This behaviour was observed due to the temporal exposure of molecules to hot spots with one part, followed by exposure with another, and exiting the pore. Since the time the molecule stays attached is random, the length of the relative regions on the waterfall graphs might differ. Apart from that, since the molecule is exposed only with a certain side to the hot spot, only some of the Raman peaks might be enhanced. The blinking of the signal may be explained by the “stop-and-go” mechanism in which the molecule temporarily contacts the metallic surface that followed by its rapid detachment after a few microseconds.

While such long translocation events are relatively rare, they serve as representative examples that clearly illustrate the mechanism and feasibility of molecular sequencing in our system. These events provide essential insight into the sequential exposure of different molecular segments to the plasmonic hotspot, resulting in distinguishable spectral signatures. However, most events occur at higher translocation speeds and emit a lower number of photons, making visual segmentation infeasible. To overcome this limitation and extract

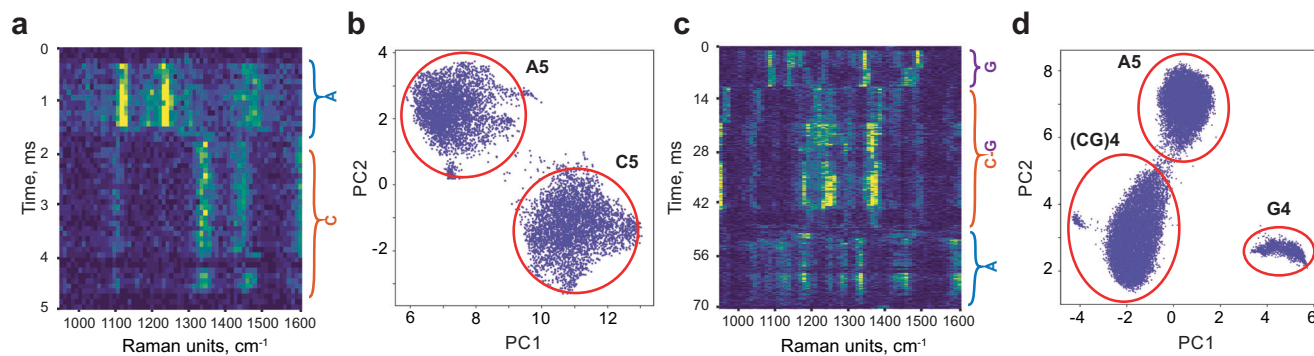


**Fig. 4 | Waterfall Spectra and PCA analyses showing spatial resolution along the molecule backbone.** Frame-level SERS analysis of A5C5 (**a, b**) and A5C(CG)4AG4 (**c, d**). **a, c** Waterfall graphs of single-molecule translocation events with long dwell times, showing distinct spectral domains for separate sequence blocks of the

molecules. **b, d** UMAP projections of the full frame-by-frame SERS datasets, illustrating clustering of distinct sequence blocks across multiple translocation events along PC1 and PC2.

structural information from the broader dataset, we applied advanced analytical methods. Figure 4b, d present the results of UMAP dimensionality reduction applied to the full set of frames from all translocation events of A5C5 and A5C(CG)4AG4. This approach demonstrates clear clustering, with the number of distinct clusters corresponding to the number of blocks in each molecule. The assignment of clusters to specific molecular segments was confirmed by comparing their spectral features, presented in Figure S9, with single-nucleotide spectra. Notably, although the Raman spectra of nucleotide chains resemble those of single nucleotides, they exhibit additional complexity arising from inter-nucleotide interactions and chain conformation, which contributes to the observed block-level differentiation. In this regard, it would be beneficial to better evaluate the optimal pore size and make the pore size more uniform. However, we think these results clearly state the possibility of distinguishing between the blocks of a studied molecule, making the sequence idea possible, using the advanced data analysis approaches.

Notably, biological pores with electrical readout can assess the nucleotide sequence with a resolution of 4–7 units due to the longitudinal size of biological pores. According to Fig. 4, the spatial resolution achieved in our experiments is at least 5 nucleotides. However, considering the sharp transition observed from A to C, it is reasonable to think that the real spatial resolution is better than 5 nucleotides, hence  $\leq 17$  Å. This agrees with pioneer works on extremely confined plasmonic hot spots further enhanced by atomic dislocation or adatoms<sup>9,16</sup> or similar effects generated in Tip-Enhanced Raman Spectroscopy combined with a scanning tunneling microscope<sup>28</sup>, photochemical reaction mediated by tip-enhanced plasmons at sub-molecular level<sup>29</sup>.

## Discussion

Further investigations are necessary to better understand many aspects of this technology that is still in its infancy, and of course, many optimizations are necessary in every direction, including optical setups and SPAD cameras, plasmonic pores, electrophoretic translocation protocols, and data analyses. However, considering the data presented here, combined with the immense literature on SERS and nanopore technologies, several conclusions can be drawn. The performance of SPAD cameras is improving at a remarkable rate, with the number of pixels rapidly increasing due to the recent adoption of scaled 3D-stacked technologies for SPAD arrays, which allow for reduced pixel pitch and power consumption while improving the SPAD detection efficiency<sup>30</sup>. Hence, Raman analyses at unprecedented speed will soon be a reality. However, to make all this suitable for practical applications, effective and affordable SERS substrates are needed, possibly allowing for flow-through settings. In this context,

permeable plasmonic films is a formidable opportunity. They are inexpensive, mechanically robust, and easy to produce for single-time use. During our experiments, which lasted under 3 h each, the silver coating and agarose gel remained intact at the applied voltage. Generated plasmonic hot spots enhance Raman scattering to an intensity that makes feasible the identification of nucleotides within the microsecond translocation time based on their single-molecule spectra with 89% accuracy using machine learning. Averaging spectra acquired, we can discriminate the nucleosides with more precision by looking at their key differences, thus confirming the power of the Raman fingerprint. This allows us to assume that by accumulating only informative photons from the oscillations of molecular moieties, only with a few tens events, reliable information about the molecule may be obtained with >99% accuracy in classification (Supplementary Note 9). Despite the very low concentration used (1 nM) the acquisition takes a few minutes thanks to a highly effective capture rate. These numbers can improve a lot, considering that the current efficiency of our optical setup enables the recording of 1 photon over 10 scattered. There is significant room for improvements that can increase accuracy and both temporal and spatial resolution, which are correlated - shorter integration times mean higher spatial resolution. The latter depends also on the size of plasmonic hot spots. In this regard, the presented data show that plasmonic hot spots generated in permeable films provide the spatial resolution to discriminate the sequence of the nucleotides with a resolution of at least 5 units or better. Such a value is comparable to that of biological pores with electrical readout<sup>31</sup>.

Although still in its infancy, the proposed method demonstrates the feasibility of Raman-based biomolecular identification via sequential readout of functional groups, with applications extending beyond DNA sequencing. Given the comparable sizes of AAs and nucleosides, as well as the similar translocation behavior of linearized peptides and ssDNA, protein identification emerges as a promising direction. Notably, a large fraction of the human proteome is known and publicly available. Even a partial knowledge of its molecular sequence is enough to identify a protein of interest. For instance, sequencing only two of 20 AA types in total is sufficient to identify over 90% of human proteins by database matching<sup>32,33</sup>. Furthermore, this approach is not limited to linear biomolecules, offering broader applicability.

## Data availability

The data is available from the corresponding author upon request.

## Code availability

The code used for data processing is available from the corresponding author upon request.

## References

1. Itoh, T. et al. Toward a New Era of SERS and TERS at the Nanometer Scale: From Fundamentals to Innovative Applications. *Chem. Rev.* **123**, 1552–1634 (2023).
2. Bi, X., Czajkowsky, D. M., Shao, Z. & Ye, J. Digital colloid-enhanced Raman spectroscopy by single-molecule counting. *Nature* **628**, 771–775 (2024).
3. Dubey, A. et al. Demonstration of a Superior Deep-UV Surface-Enhanced Resonance Raman Scattering (SERRS) Substrate and Single-Base Mutation Detection in Oligonucleotides. *J. Am. Chem. Soc.* **143**, 19282–19286 (2021).
4. Kneipp, J., Seifert, S. & Gärber, F. SERS microscopy as a tool for comprehensive biochemical characterization in complex samples. *Chem. Soc. Rev.* **53**, 7641–7656 (2024).
5. Lee, S. et al. SERS-based microdevices for use as in vitro diagnostic biosensors. *Chem. Soc. Rev.* **53**, 5394–5427 (2024).
6. Bennett, H. M., Stephenson, W., Rose, C. M. & Darmanis, S. Single-cell proteomics enabled by next-generation sequencing or mass spectrometry. *Nat. Methods* **20**, 363–374 (2023).
7. Ying, Y. L. et al. Nanopore-based technologies beyond DNA sequencing. *Nat. Nanotechnol.* **17**, 1136–1146 (2022).
8. Dorey, A. & Howorka, S. Nanopore DNA sequencing technologies and their applications towards single-molecule proteomics. *Nat. Chem.* **16**, 314–334 (2024).
9. Zhang, Y., Lu, L. & Li, X. Detection technologies for RNA modifications. *Exp. Mol. Med.* **54**, 1601–1616 (2022).
10. Li, W. et al. High-Throughput Single-Molecule Surface-Enhanced Raman Spectroscopic Profiling of Single-Amino Acid Substitutions in Peptides by a Gold Plasmonic Nanopore. *ACS Nano* **18**, 19200–19207 (2024).
11. Chen, C. et al. High spatial resolution nanoslit SERS for single-molecule nucleobase sensing. *Nat. Commun.* **9**, 1–9 (2018).
12. Iarossi, M. et al. High-Density Plasmonic Nanopores for DNA Sensing at Ultra-Low Concentrations by Plasmon-Enhanced Raman Spectroscopy. *Adv. Funct. Mater.* **33**, 2301934 (2023).
13. Zhao, Y. et al. Plasmonic Bowl-Shaped Nanopore for Raman Detection of Single DNA Molecules in Flow-Through. *Nano Lett.* **23**, 4830–4836 (2023).
14. Huang, J. A. et al. SERS discrimination of single DNA bases in single oligonucleotides by electro-plasmonic trapping. *Nat. Commun.* **10**, 1–10 (2019).
15. Soni, N., Chandra Verma, N., Talor, N. & Meller, A. Over 30-Fold Enhancement in DNA Translocation Dynamics through Nanoscale Pores Coated with an Anionic Surfactant. *Nano Lett.* **23**, 4609–4616 (2023).
16. Goto, Y., Akahori, R., Yanagi, I. & Takeda, K. Solid-state nanopores towards single-molecule DNA sequencing. *J. Hum. Genet.* **65**, 69–77 (2019).
17. Borah, R., Ninakanti, R., Bals, S. & Verbruggen, S. W. Plasmon resonance of gold and silver nanoparticle arrays in the Kretschmann (attenuated total reflectance) vs. direct incidence configuration. *Sci. Rep.* **12**, 1–19 (2022).
18. Dadadzhyanov, D. R., Gladskikh, I. A., Baranov, M. A., Vartanyan, T. A. & Karabchevsky, A. Self-organized plasmonic metasurfaces: The role of the Purcell effect in metal-enhanced chemiluminescence (MEC). *Sens Actuators B Chem.* **333**, 129453 (2021).
19. Shan, F. et al. Investigation of simultaneously existed Raman scattering enhancement and inhibiting fluorescence using surface modified gold nanostars as SERS probes. *Sci. Rep.* **7**, 1–10 (2017).
20. Baumberg, J. J., Aizpurua, J., Mikkelsen, M. H. & Smith, D. R. Extreme nanophotonics from ultrathin metallic gaps. *Nat. Mater.* **18**, 668–678 (2019).
21. Benz, F. et al. Single-molecule optomechanics in ‘picocavities’. *Science* (1979) **354**, 726–729 (2016).
22. Lindquist, N. C., de Albuquerque, C. D. L., Sobral-Filho, R. G., Paci, I. & Brolo, A. G. High-speed imaging of surface-enhanced Raman scattering fluctuations from individual nanoparticles. *Nat. Nanotechnol.* **14**, 981–987 (2019).
23. Schmidt, M. M., Brolo, A. G. & Lindquist, N. C. Single-Molecule Surface-Enhanced Raman Spectroscopy: Challenges, Opportunities, and Future Directions. *ACS Nano* <https://doi.org/10.1021/ACS.NANO.4C09483> (2024).
24. Emmerich, T. et al. Nanofluidics. *Nat. Rev. Methods Prim.* **4**, 1–18 (2024).
25. Feng, J. et al. Identification of single nucleotides in MoS<sub>2</sub> nanopores. *Nat. Nanotechnol.* **10**, 1070–1076 (2015).
26. Bruno, G. et al. Label-Free Detection of Biochemical Changes during Cortical Organoid Maturation via Raman Spectroscopy and Machine Learning. *Anal. Chem.* **14**, 59 (2025).
27. Altug, H., Oh, S. H., Maier, S. A. & Homola, J. Advances and applications of nanophotonic biosensors. *Nat. Nanotechnol.* **17**, 5–16 (2022).
28. Jacubcia, R. B. et al. Single-molecule resonance Raman effect in a plasmonic nanocavity. *Nat. Nanotechnol.* **15**, 105–110 (2020).
29. Rostawska, A. et al. Submolecular-scale control of photo-tautomerization. *Nat. Nanotechnol.* **19**, 738–743 (2024).
30. Wojtkiewicz, M., Rae, B. & Henderson, R. K. Review of Back-Side Illuminated 3-D-Stacked SPADs for Time-of-Flight and Single-Photon Imaging. *IEEE Trans. Electron Devices* **71**, 3470–3477 (2024).
31. Lu, C., Bonini, A., Viel, J. H. & Maglia, G. Toward single-molecule protein sequencing using nanopores. *Nat. Biotechnol.* **2025**, 1–11 <https://doi.org/10.1038/s41587-025-02587-y> (2025).
32. Yao, Y., Docter, M., Van Ginkel, J., De Ridder, D. & Joo, C. Single-molecule protein sequencing through fingerprinting: computational assessment. *Phys. Biol.* **12**, 055003 (2015).
33. Meller, A., Ohayon, S., & Girsault, A. Machine learning for protein identification. Patent WO2020084619A1 (2022).

## Acknowledgements

This work is dedicated to Aliaksandr Hubarevich, beloved scientist and colleague, passed away during the preparation of the manuscript. He provided the theoretical and computational support for the conception and execution of the work. We acknowledge funding of this research by the European Union’s Horizon 2020 Programme- Grant Agreement n. 964363 “ProID” - H2020-FETOPEN-2018-2020. Nick Goldman was supported by the European Molecular Biology Laboratory (EMBL). We acknowledge support from MPD (Micro Photon Devices) Company for providing the SPAD Camera. More info at [www.micro-photon-devices.com](http://www.micro-photon-devices.com). We acknowledge support from DifiLab (under the project “Dipartimenti di Eccellenza 2018–2022” of the Italian Ministry of Education), granting access to JPK. We acknowledge prof. Claudio Canale from Università di Genova for providing support and valuable discussion.

## Author contributions

K.K. performed Raman experiments and analysed data. M.B.F., I.M.B., F.K.S. fabricated samples. R.M. helped with the optical setup. G.B., B.B., F.G., N.G. contributed to data analyses. V.S., H.H., F.V. developed the SPAD camera and interfaces. P.C. performed AFM analyses. N.G., F.V., M.D., F.T., F.D.A. supervised the work. F.D.A. conceived the original idea and coordinated the whole project.

## Competing interests

The authors declare no competing interests.

## Additional information

**Supplementary information** The online version contains supplementary material available at <https://doi.org/10.1038/s41467-025-64165-9>.

**Correspondence** and requests for materials should be addressed to Francesco Tantussi or Francesco De Angelis.

**Peer review information** *Nature Communications* thanks anonymous reviewers for their contribution to the peer review of this work. [A peer review file is available.]

**Reprints and permissions information** is available at <http://www.nature.com/reprints>

**Publisher's note** Springer Nature remains neutral with regard to jurisdictional claims in published maps and institutional affiliations.

**Open Access** This article is licensed under a Creative Commons Attribution-NonCommercial-NoDerivatives 4.0 International License, which permits any non-commercial use, sharing, distribution and reproduction in any medium or format, as long as you give appropriate credit to the original author(s) and the source, provide a link to the Creative Commons licence, and indicate if you modified the licensed material. You do not have permission under this licence to share adapted material derived from this article or parts of it. The images or other third party material in this article are included in the article's Creative Commons licence, unless indicated otherwise in a credit line to the material. If material is not included in the article's Creative Commons licence and your intended use is not permitted by statutory regulation or exceeds the permitted use, you will need to obtain permission directly from the copyright holder. To view a copy of this licence, visit <http://creativecommons.org/licenses/by-nc-nd/4.0/>.

© The Author(s) 2025